Acta Cryst. (1985). B41, 362-368

Molecular-Replacement Structure of Guinea Pig IgG1 pFc′ Refined at 3·1 Å Resolution

BY S. H. BRYANT

Department of Biostatistics, Johns Hopkins University, School of Hygiene and Public Health, 615 N. Wolfe St, Baltimore, MD 21205, USA

L. M. AMZEL

Department of Biophysics, Johns Hopkins University, School of Medicine, 725 N. Wolfe St, Baltimore, MD 21205, USA

R. P. PHIZACKERLEY

Department of Structural Biology, Stanford University, Stanford, CA 94305, USA

AND R. J. POLJAK

Immunologie Structurale, Institut Pasteur, 28 rue du Dr Roux, 75724 Paris CEDEX 15, France

(*Received* 20 *August* 1984; *accepted* 22 *May* 1985)

Abstract

The structure of guinea pig IgG1 pFc′ fragment has been refined with 3·1 Å X-ray diffraction data to a final R of 0·30 ($R = 30\%$ for 95% of the possible reflections; $R = 25\%$ for the 75% strongest reflections) using a combination of difference Fourier, real-space and restrained least-squares refinement techniques. The commonly used procedures were modified to employ a correction for bulk solvent contribution to F_c, and an F_o weighting scheme designed to equalize $\langle w(F_o - F_c)^2 \rangle$ for all intervals of F_o and s. The refined model is quite different from the molecular-replacement probe used for phasing, and demonstrates that macromolecular refinement techniques can correct errors in the initial model using only medium-resolution data. The final model does not appear to be heavily biased towards the probe structure. Amino acid residues implicated in biological function are on the molecular surface. Some structural differences between guinea pig IgG pFc′ and human IgG Fc may reflect adaptation to packing constraints imposed by the crystal lattice.

Introduction

The physical basis for immunoglobulin antigen binding specificity has been defined by crystallographic studies of immunoglobulin fragments and fragment-ligand complexes (Amzel & Poljak, 1979). Secondary activities such as complement activation and anaphylaxis involve binding of aggregated immunoglobulin (Metzger, 1978) with other macromolecules (Feutrell *et al.*, 1979), and the precise molecular mechanisms of these activities remain obscure. Guinea pig IgG1 is active in assays for anaphylaxis in the guinea pig, and most studies suggest that the receptor binding site responsible for this activity falls in the Fc region, and possibly within the C_H3 homology subunit, corresponding to pFc′ (Ovary, 1978; Alexander, Andrews, Leslie & Wood, 1978). We have undertaken the present work in the belief that the refined pFc′ coordinates will contribute towards understanding the mechanisms of this activity.

The pFc′ structure was previously solved using the refined coordinates of a human IgG C_H1 subunit as a molecular-replacement probe (Phizackerley, Wishner, Bryant, Amzel, Lopez de Castro & Poljak, 1979). The amino acid sequence homology between these proteins is only 23%. To our knowledge no other protein structure has been solved using a probe as dissimilar as this. It is of interest to know to what extent the pFc′ structure can be considered independent of the probe, and to what extent refinement has overcome the systematic bias introduced by molecular-replacement phases.

The currently available pFc′ diffraction data extend to only 3·1 Å resolution, where many details of polypeptide conformation cannot be seen in electron density maps. In this paper we refined the initial pFc′ model using a combination of difference Fourier and automatic refinement techniques, which we have adapted to make the best use of low- and medium-resolution data. Two novel features were a correction for bulk displaced solvent and a weighting scheme for restrained least-squares refinement that was designed to equalize residuals over intervals of s and F_o. In addition to the commonly employed restrained isotropic temperature factors we included restraints on protein secondary structure, in an effort to define a model that best reflects the structural information contained in the available data set.

0108-7681/85/050362-07$01.50

Experimental

Crystallographic data

pFc′ crystallizes in space group $I422$, $a = b = 60{\cdot}57$, $c = 136{\cdot}54$ Å. There is one monomer of molecular weight 12 500 in the asymmetric unit. Diffraction data were collected with a Hilger & Watts Y290 four-circle diffractometer using 'ordinate analysis' (Phizackerley, Wishner, Brynant, Amzel, Lopez de Castro & Poljak, 1979), and consist of 2339 independent structure factors between 15 and 3·1 Å, including 1728 between 5 and 3·1 Å. Ninety-five per cent of the theoretically expected reflections were observed with significant intensity.

Structure factor calculation

During real-space refinement structure factors were calculated from atomic coordinates using programs for fast-Fourier transform by R. K. McMullan and S. T. Rao. These programs were modified to employ a synthetic atomic electron density profile best suited for Fourier inversion (Amzel & Lattman, 1979). This procedure allowed sampling of the model electron density at a grid spacing of 1·37 Å, with less than 1·5% disagreement with structure factors calculated conventionally.

A correction for displaced solvent was applied by substituting a modified atomic scattering factor $ff(s)$ in the fast-Fourier transform calculation. Here $ff(s) = f(s) - v\rho[\exp(-4\pi v^{2/3}s^2)]$ where $f(s)$ is the conventional atomic scattering factor, v is the average volume of solvent displaced by a protein atom, assumed to be 12·68 Å^3, and ρ is the electron density of the solvent (Fraser, MacRae & Suzuki, 1978), assumed to be 0·334 Å^{-3}. The subtractive term gives the scattering by displaced solvent, represented as a Gaussian sphere.

In the course of reciprocal-space refinement structure factors were calculated with a conventional formula using individual isotropic atomic temperature factors and solvent-corrected individual atomic scattering factors (Fraser, MacRae & Suzuki, 1978). For the calculation of fragment difference electron density maps partial structure factors were calculated by the same method for the region of the structure to be omitted, and the calculated structure factors were obtained by complex subtraction.

An overall temperature factor was originally determined from a Wilson plot. In scaling observed to calculated structure factors corrections for reflection multiplicity, unobserved reflections, and abnormal average intensity were performed by standard methods, using a single overall scale factor (Bryant, 1982).

Electron density map calculation

Difference electron density maps were calculated using the fast-Fourier programs written by R. K. McMullan and S. T. Rao. Structure factors with F_o greater than $3F_c$ were omitted in calculation of the maps. The transform was calculated for 64 points along **a** and **b**, 144 points along **c**. This corresponds to grid-point spacings of 0·946 and 0·948 Å, respectively. Maps were contoured onto 35 mm film using a digital filmwriter.

Rebuilding the molecular model

Sections of the electron density map were projected and traced onto Mylar sheets at 2 cm Å^{-1}. A brass wire model was constructed in an optical comparator. Atomic coordinates for all non-hydrogen atoms were measured using a mechanical device, with reproducibility to within 0·25 Å. Coordinates measured from the wire model were revised to idealize bond lengths and interbond angles using the model-building program by Diamond (1966). Optimum control parameters were determined by trials using a portion of the pFc′ structure.

The final series of difference maps was displayed and interpreted at the GRIP molecular-graphics facility at the University of North Carolina, Department of Computer Science. Changes in the model were corrected for poor geometry interactively, using the program *REFINE* written by David Tolle, with optimum control parameters determined by trial.

Real-space refinement

The model was refined against $2F_o - F_c$ maps calculated with 15 to 3·1 Å data, using the program by Diamond (1971). Control parameters appropriate to refinement at this resolution were selected by trial.

Reciprocal-space refinement

The programs *SCATT*, *PROTIN*, and *PROLSQ* by Konnert & Hendrickson (1980) were used, modified to calculate structure factors and positional derivatives in space group $I422$. The program *SCATT* was modified to utilize atomic scattering factors that include the solvent correction described above. For the second series of reciprocal-space refinement runs, *SCATT* was further modified to include calculation of a weighting factor for each reflection.

In the refinement of pFc′ a maximum of 7478 geometrical restraints were applied. Positions and, in later stages, isotropic thermal factors were refined for a maximum of 878 atoms. Geometrical residuals were weighted by $1/\sigma_g$, where σ_g is the standard deviation found in appropriate small-molecule structures. Values were provided by Konnert and Hendrickson with *PROLSQ*. For the pFc′ data set weighting structure factor residuals by $3{\cdot}4/\sigma_f$, where $\sigma_f = \langle(F_o - F_c)^2\rangle^{\frac{1}{2}}$, was found to maintain acceptable geometry and still allow improvement in R. In some later cycles structure factor weights were specified as

a linear function of s, as allowed by *PROLSQ*, with an average value of $3{\cdot}4/\sigma_f$. This weighting did not lead to a reduced R. In the final cycles of refinement structure factor weights were chosen to equalize $\langle w(F_o - F_c)^2 \rangle$ for all intervals of F_o and s. The analytical expression for $w(F_o, s)$ fitted interval $\langle (F_o - F_c)^2 \rangle$ with a cubic polynomial in $\langle F_o \rangle$ multiplied by a linear function of $\langle s \rangle$. The $(F_o - F_c)^2$ terms were then weighted in the refinement by $w(F_o, s)$.

Secondary structure restraints applied during the final stages of refinement were specified as target values for bond angles and additional bond lengths to be restrained. φ and ψ values for an ideal antiparallel β sheet were set at $-139°$ and 135°. The hydrogen-bond lengths were targeted at 2·85 Å. In the refinement of pFc′ with full secondary structure restraints 44 φ and ψ pairs were restrained, as were 33 hydrogen-bond lengths. Weighting parameters were selected empirically to balance improvement in secondary structure with distortion in other bond lengths and angles.

Both series of reciprocal-space refinement runs were begun with a single overall temperature factor. Shifts in overall temperature factor and scale factor were applied only in alternate cycles, as suggested by W. Hendrickson. Simultaneous corrections to the scale factor and average temperature factor were determined using 'Delta-B' plots, as in Fig. 4, fitted by linear regression. Individual atomic thermal factors were introduced in later cycles, initialized to the current overall temperature factor.

Crystal-packing contacts

Packing contacts including contacts due to dimer and other crystal symmetry were analyzed using the programs *CONTAX* and *LISTNG* written by Eduardo Padlan.

Molecular structure comparisons

The α carbon coordinates for pFc′ were compared to those for human C_H1 and unrefined pFc′ using the program *HOMOGR* written by S. T. Rao and M. Rossmann. Human Fab New C_H1 coordinates were those reported by Saul, Amzel & Poljak (1978). Comparison to human IgG1 Fc C_H3 region was done using the program *ALIGN* by L. M. Amzel, which also produced rotated and translated Fc coordinates that could be used for packing analysis of Fc C_H3 in the pFc′ lattice. Coordinates for refined Fc were kindly provided by J. Deisenhofer.

Computing facilities

Fast-Fourier transform calculations and real-space refinement were performed on the CDC 7600 computer at Brookhaven National Laboratory. Reciprocal-space refinement was carried out on the Texas Instruments ASC computer at the Naval Research Laboratory, Washington, DC.

Results

Refinement strategy

The original model was partially rebuilt against $F_o - F_c$ and $2F_o - F_c$ maps, which were not interpretable in some regions. A single cycle of real-space refinement was carried out against the $2F_o - F_c$ map. The model was then completely rebuilt against a series of fragment $2F_o - F_c$ maps. In any one map regions spanning 10 to 15 residues were omitted from the F_c calculation. The resulting model was refined to convergence using first the real-space and then the reciprocal-space least-squares technique. This model was then rebuilt again against fragment $2F_o - F_c$ maps, and refined to convergence using the reciprocal-space least-squares technique.

Progress of the refinement

In the first complete round of rebuilding the interpretation of the map was extended using several additional residues so that amino acids R334 to G446, the entire pFc′ sequence, were included in the interpretation. The partially exposed bends at L350 to S364 and K411 to F423 appeared to have been traced incorrectly, and they were re-interpreted. These and the exposed bends at D382 to Y391, G371 to A375, D399 to S403 and H429 to H435 were modified slightly in rebuilding against the second series of $2F_o - F_c$ maps. Reinterpretation of the density corresponding to conserved β-sheet regions was not suggested by any of the maps.

The overall course of the refinement is summarized in Fig. 1. Automatic refinement had clearly converged after each round of model building, as further reductions in the crystallographic R could not be obtained without relaxed geometry. A third set of fragment $2F_o - F_c$ maps was calculated and examined, but no significant re-interpretation of the density was possible, and refinement using the current data set is considered complete.

Comparison to the molecular-replacement probe

The initial pFc′ model (Phizackerley, Wishner, Bryant, Amzel, Lopez de Castro & Poljak, 1979) tended to reproduce the human C_H1 probe structure. α carbon coordinates for 84 out of 98 pFc′ residues fell within 1·5 Å of the corresponding C_H1 residues. For the refined structure 61 out of 111 α carbon atoms fell within 1·5 Å of the corresponding C_H1 atoms, or 77 out of 111 within 3·0 Å. The residues which changed positions least during refinement fall entirely within the conserved β-sheet secondary structure. Stereodiagrams of the human C_H1 probe, the initial

pFc′ model, and the refined pFc′ structure are shown in Fig. 2.

pFc′ secondary structure

The hydrogen-bonding pattern present in the original model was retained throughout refinement. In the final stage of automatic refinement the pFc′ β-sheet structure was analyzed quantitatively, with the results shown in Table 1. Since the deviation from ideal geometry had increased, restraints on secondary structure parameters were introduced for the remaining cycles of automatic refinement. Restraints had the effect of restoring a more ideal geometry, without a significant increase in the crystallographic *R*. The r.m.s. coordinate shift of 0·26 Å resulting from these restraints is in fact an estimate of the maximum precision of the pFc′ coordinate set.

Atomic temperature factors

Individual atomic temperature factors were refined during the final cycles of reciprocal-space refinement, with restraints forcing similar values within regions along the peptide chain. The refined values are generally higher for residues in bend regions and on the molecular surface, as shown in Fig. 3. These regions were less well defined in the maps, and the temperature factor results we report quantify this observation.

Table 1. *Analysis of pFc′ β-sheet structure before and after application of restraints*; *residues included in the table and whose conformation was restrained are*: 347–350, 365–371, 377–381, 391–394, 397–399, 403–410, 418–420 (*helical*), 423–429, 434–439

	φ	ψ	H-bond length
Ideal antiparallel β sheet	−139°	135°	2·85 Å
Initial pFc′ model	−121 ± 38	131 ± 31	3·25 ± 0·48
After refinement with no restraints	−136 ± 49	140 ± 42	3·58 ± 0·83
After further refinement with restraints	−135 ± 24	140 ± 29	3·21 ± 0·40

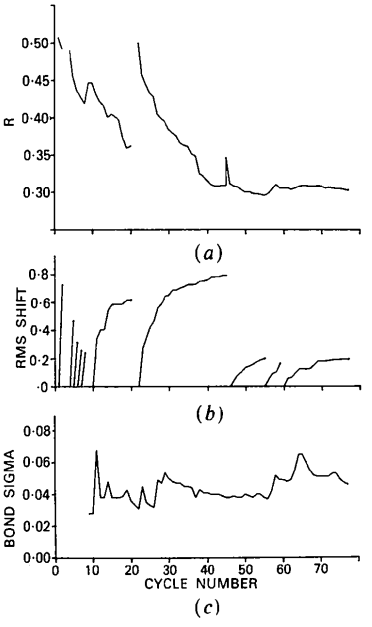

Fig. 1. Progress of refinement. Each automatic refinement run or manual model rebuilding is designated a cycle. (*a*) The decrease in crystallographic *R*. (*b*) The r.m.s. coordinate shift produced by each automatic refinement run, expressed as a cumulative shift for reciprocal-space refinement runs with identical restraints. (*c*) The standard deviation in C-C bond lengths with respect to ideal values, as an indication of overall model geometry. Manual model building was done at cycles 0, 3, and 21, real-space automatic refinement at cycles 1 and 4 to 6, reciprocal-space refinement at cycles 7 to 20 and 22 to 77. Individual atomic thermal factors were refined between cycles 13 to 20 and 33 to 77. Weighting F_o data as a function of s was introduced for cycles 17 to 20 and 33 to 46. Weighting factors designed to equalize $\langle(F_o - F_c)^2\rangle$ for ranges of F_o and s were introduced for cycles 49 to 77. Secondary structure restraints were introduced for cycles 55 to 77. Cycles 1 to 36 used 15 to 3·1 Å data; cycles 37 to 77 used 5 to 3·1 Å data.

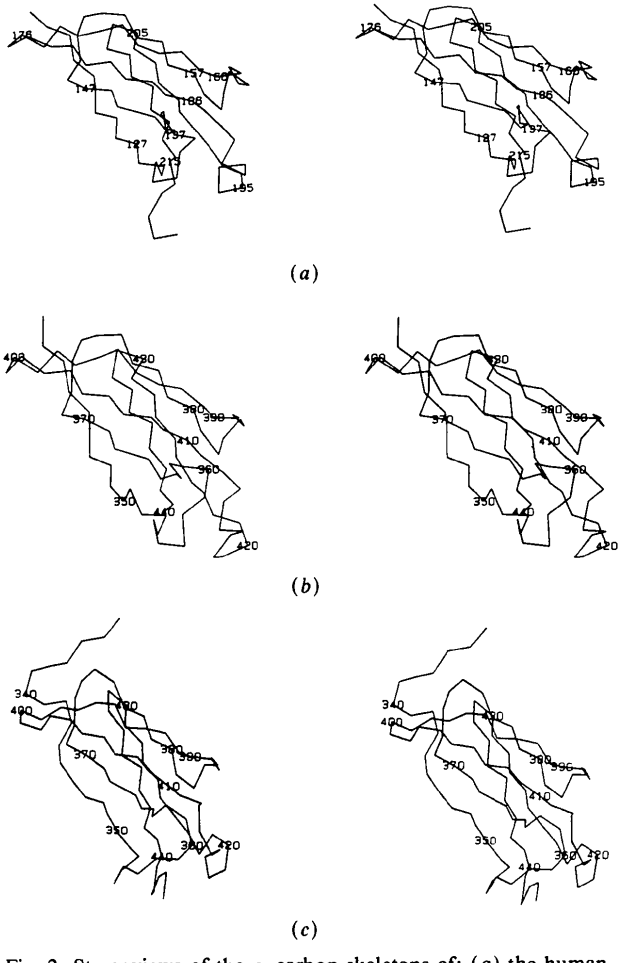

Fig. 2. Stereoviews of the α carbon skeletons of: (*a*) the human C_H1 probe, (*b*) the initial pFc′ model, and (*c*) the refined pFc′ structure.

Analysis of crystal-packing contacts

In the pFc′ crystal the molecular dimer axis coincides with a crystallographic twofold axis at $x = 0{\cdot}5, y = 0$. The pattern of contacts resembles the $C_H1 - C_L$ contacts in human Fab (Amzel & Poljak, 1979) as would be expected on the basis of overall structural homology. Overall, there were 285 atom-to-atom dimer contacts at less than 1·2 times the sum of the van der Waals radii. Only 38 were shorter than 0·8 times this distance, and 6 were shorter than 0·6 times this distance. Of 105 contacts produced by other symmetry elements 12 were shorter than 0·8 times the sum of the van der Waals radii, and 2 less than 0·6 times this distance. The number of contacts which are too close is consistent with the imprecision of the refined coordinates indicated in the analysis of secondary structure. That there are not more close contacts suggests the model defines the molecular surface accurately, since packing geometry was not restrained in the automatic refinement procedures.

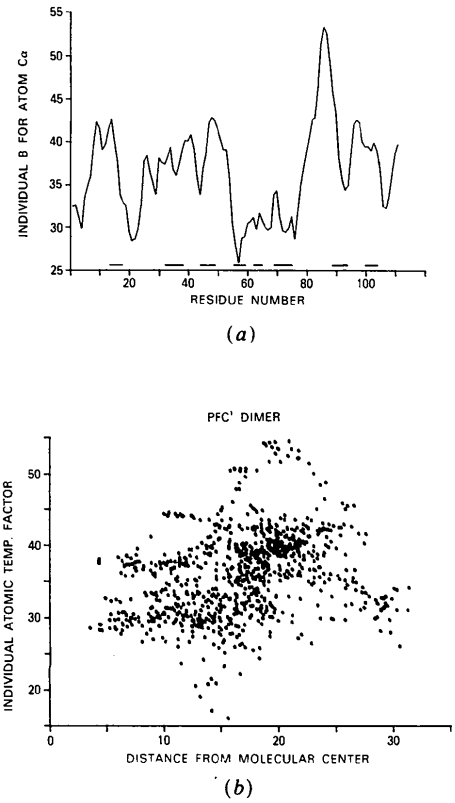

Fig. 3. (*a*) Individual atomic thermal factors (Å^2) for pFc′ α carbons, where regions of conserved β-sheet structure are designated by a horizontal bar. pFc′ residue 1 corresponds to position 334 in the IgG Eu numbering system, where residues 385 and 386 are considered to be deleted in guinea pig IgG1. (*b*) Individual atomic thermal factors (Å^2) and the distance of the corresponding atom from the molecular center (Å).

Comparison to human Fc structure

Forty-four out of 111 pFc′ α carbon coordinates fall within 1·5 Å of the corresponding atoms in Fc, with an average distance of 0·80 Å. This degree of similarity supports the hypothesis that the C_H3 region structure is highly conserved between species and between immunoglobulin subclasses, as has been suggested on the basis of sequence data.

There are three regions where guinea pig pFc′ and human Fc differ consistently by more than 1·0 Å. These are the bend at residues 382–390, the bend at residues 430–435, and the strand of β sheet from residues 436–440. There are also large differences for nine residues at the N-terminus, which forms part of C_H2 in intact IgG1, and five residues at the C-terminus, which falls outside the globular region. We suspect the conformations of these last two regions reflect packing constraints peculiar to the pFc′ crystals, since they are not in tight contact with the rest of the molecule, and yet are constrained by symmetry-related molecules within the unit cell.

In pFc′ the bend at residues 382–390 is two residues shorter than in Fc, and there are six amino acid differences among the seven residues. The bend structure of pFc′ resembles the structure seen in human C_H1, and in Fc this bend more resembles the structure seen in human C_L. The bend structure seen in Fc is not compatible with the pFc′ lattice, as impossible packing contacts to the region 357–363 and the residues 413, 401 and 371 would result. While we cannot rule out the possibility of errors in interpretation of medium-resolution electron density maps, the sequence differences and packing considerations also suggest there are real structural differences in this region.

The bend at pFc′ residues 430–435 is located near the fourfold rotation axis of space group *I*422. In this lattice the Fc structure would form impossible contacts *via* the fourfold axis. It seems possible the structural differences in this region reflect a conformational change in pFc′ caused by pepsin cleavage and crystallization, since these residues form C_H2 contacts in Fc, and intermolecular packing contacts in pFc′ crystals. This hypothesis is in agreement with circular-dichroism observations by Ellerson, Yasmeen, Painter & Dorrington (1976) who conclude that conformational changes accompany cleavage of Fc between C_H3 and C_H2.

The β strand at residues 436–440 appears to be out of phase by one residue between pFc′ and Fc. It seems likely that this difference reflects difficulties in interpretation of the density maps. This short strand is bracketed by the bend at residues 430–435, and the C-terminal residues, which differ in structure, and it is also possible the shift in position for the intervening strand of β sheet reflects a conformational change resulting from cleavage and crystallization.

Discussion

Refinement of the molecular-replacement structure

A molecular-replacement structure is systematically biased towards the probe used for phasing. One would like to know how much, and to what extent macromolecular refinement techniques can correct this bias.

The refined pFc′ structure was compared with the C_H1 probe and with human Fc, and found to have strong similarities to both structures. The similarity to C_H1 is probably higher than expected from their sequence homology. This comparison is complicated, however, by the higher resolution of the C_H1 probe structure and possible conformational changes in pFc′ due to pepsin cleavage and crystal packing. During refinement the pFc′ structure has become less similar to C_H1 as shown in Fig. 2, and this was accompanied by a decrease in R. Clearly the information contained in the F_o data has tended to counteract bias in the initial model. The final R of 0·30 appears to be higher than those obtained in the refinement at similar resolution of a human IgG V_L dimer (Furey, Wang, Yoo & Sax, 1979) and human IgG Fc (Deisenhofer, 1981), which were solved by the MIR method. The pFc′ data set, however, includes nearly all reflections, and if only the strongest 75% of the theoretically expected reflections are considered R is 0·25, which is as low as was obtained in the MIR structures available. The geometrical quality of the pFc′ structure does not seem unusual for a 3·1 Å structure, as shown by the data on bond lengths, secondary structure, and packing contacts. Based on these considerations we conclude that the errors remaining in the pFc′ structure are probably no larger than in MIR structures refined at this resolution, but refinement at higher resolution would constitute a more conclusive test.

Using low- and medium-resolution data in refinement

Reflections below 5 Å are commonly omitted from difference map calculation and least-squares refinement because of scaling artifacts and large contributions to the least-squares sum by long-angle $F_o - F_c$ terms. These data constitute 26% of the pFc′ data set, and with this in mind we adopted the solvent-correction technique, which allowed us to use these data. As shown in Fig. 4 the displaced solvent correction made scaling by shells unnecessary, as it apparently models successfully the contribution of solvent in the unit cell to the low-resolution reflections. These data were used until the final cycles of restrained least-squares refinement, as shown in Fig. 1.

During the final stages of least-squares refinement we noted that the higher-intensity reflections were contributing disproportionately to the overall residual. An example of the weighting scheme we employed to correct this problem is shown in Fig. 5, which shows specifically the weighted and unweighted sums of squared residuals for the final cycle of refinement. This weighting scheme successfully equalized the contributions of the low- and high-intensity reflections to the total sum of squares. The F_o weighting procedure improved the contribution of these data to the structure, since R dropped by 0·01

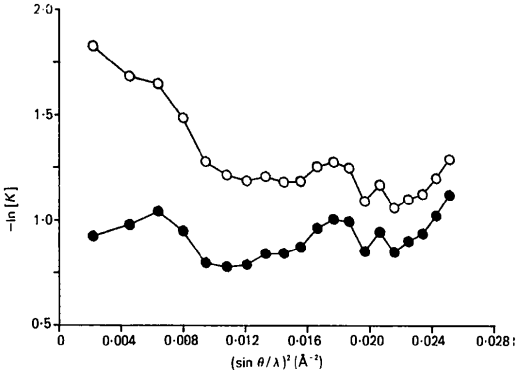

Fig. 4. Plot of calculated shell scale factors before (open circles) and after (solid circles) F_c calculation with solvent correction.

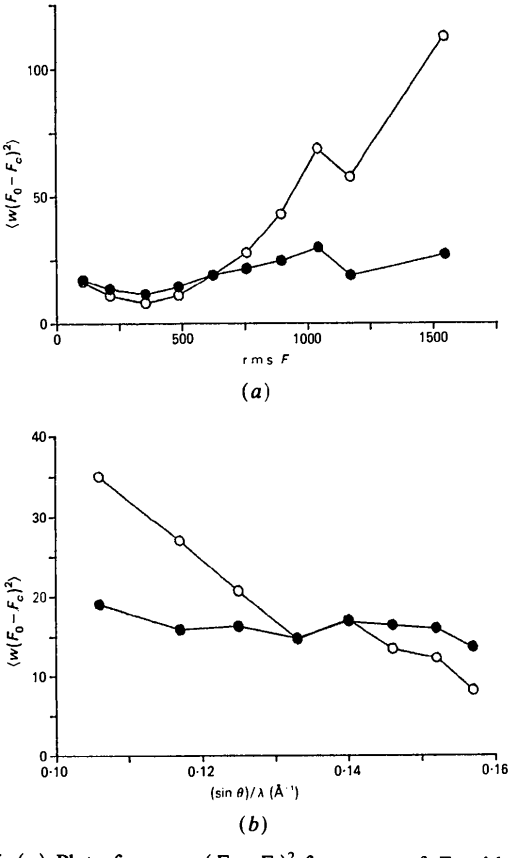

Fig. 5. (*a*) Plot of mean $w(F_o - F_c)^2$ for ranges of F_o with w a constant (open circles) *vs* w a function of F_o and s (solid circles). (*b*) Plot of mean $w(F_o - F_c)^2$ for shells of s with w a constant (open circles) *vs* w a function of F_o and s (solid circles).

compared to the model obtained when weighting with a constant factor.*

Sites essential for biological activity

Immunoglobulin effector functions are mediated by binding to other macromolecular species. The sequence changes that reflect evolution of distinct biological functions are most likely those which alter the chemical characteristics of the molecular surface. For the IgG C_H3 region such residues are largely concentrated in the long surface bends at positions 382–390 and 411–422. Fig. 6 shows the guinea pig IgG1 C_H3 solvent-exposed residues not conserved in guinea pig IgG2, which is inactive in anaphylaxis (Ovary, Benacerraf & Bloch, 1963; Oliveira, Osler, Siraganian & Sandberg, 1970), plotted on an α-carbon drawing of the pFc′ dimer. The non-homologous bend regions form a single face of the monomer which is symmetrically disposed across the dimer axis, with a separation of about 60 Å and a distance from the C-terminal face of about 20 Å. The non-homologous residues within these bends are predominantly polar residues. It has been suggested (Burton *et al.*, 1980) that the complement component C1q binding site on C_H2 is formed by an array of hydrophilic residues, and it is possible that this is the case as well for C_H3 binding to cell surface receptors.

* Atomic parameters of the refined pFc′ model and structure factors have been deposited with the Protein Data Bank, Brookhaven National Laboratory (Reference: 1PFC and R1PFCSF), and are available in machine-readable form from the Protein Data Bank at Brookhaven or one of the affiliated centers at Cambridge, Melbourne or Osaka. The data have also been deposited with the British Library Lending Division as Supplementary Publication No. SUP 37015 (2 microfiche). Free copies may be obtained through The Executive Secretary, International Union of Crystallography, 5 Abbey Square, Chester CH1 2HU, England.

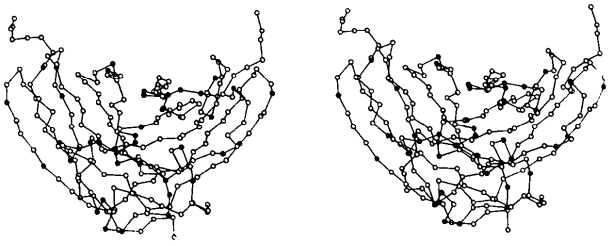

Fig. 6. Stereoview of pFc′ dimer α carbon skeleton. Positions which are non-homologous between guinea pig IgG1 and IgG2 and are exposed to solvent are designated by solid circles.

This work was supported by Research Grant AI08202 and AI20293 from the National Institutes of Health. SHB acknowledges support from NIH Training Grant GM 00184. We thank the staff of the GRIP system, supported by NIH grant RR00898, for help with molecular graphics. We thank Dr W. Hendrickson for advice and assistance with reciprocal-space refinement and J. Deisenhofer for the Fc coordinates.

References

ALEXANDER, M. D., ANDREWS, J. A., LESLIE, R. G. Q. & WOOD, N. J. (1978). *Immunology*, **35**, 115–124.

AMZEL, L. M. & LATTMAN, E. L. (1979). Personal communication.

AMZEL, L. M. & POLJAK, R. J. (1979). *Annu. Rev. Biochem.* **48**, 961–997.

BRYANT, S. H. (1982). *Crystallographic Refinement of Guinea Pig IgG1 pFc′ Fragment at 3·125 Ångströms Resolution.* PhD thesis, Johns Hopkins Univ., Baltimore.

BURTON, D. R., BOYD, J., BRAMPTON, S. B., EASTERBROOK-SMITH, S. B., EMANUEL, E. J., NOVOTNY, J., RADEMACHER, T. W., VAN SCHRAVENDIJK, M. R., STERNBERG, M. J. E. & DWEK, R. A. (1980). *Nature (London)*, **288**, 338–344.

DEISENHOFER, J. (1981). *Biochemistry*, **20**, 2362–2370.

DIAMOND, R. (1966). *Acta Cryst.* **21**, 253–266.

DIAMOND, R. (1971). *Acta Cryst.* A**27**, 436–452.

ELLERSON, J. R., YASMEEN, D., PAINTER, R. H. & DORRINGTON, K. J. (1976). *J. Immunol.* **116**, 510–517.

FEUTRELL, C., GEIER, M., GOETZE, A., HOLOWDA, D., ISENMAN, D., JONES, J. F., METZGER, H., NAVIA, M., SIECKMANN, D., SILVERTON, E. & STEIN, K. (1979). *Mol. Immunol.* **16**, 741–754.

FRASER, R. D. B., MACRAE, T. P. & SUZUKI, E. (1978). *J. Appl. Cryst.* **11**, 693–694.

FUREY, W., WANG, B. C., YOO, C. S. & SAX, M. (1979). *Acta Cryst.* A**35**, 810–817.

KONNERT, J. H. & HENDRICKSON, W. (1980). *Acta Cryst.* A**36**, 344–350.

METZGER, H. (1978). *Contemporary Topics in Molecular Immunology*, Vol. 7, edited by R. A. REISFELD & F. P. INMAN, pp. 119–152. New York: Plenum.

OLIVEIRA, B., OSLER, A. G., SIRAGANIAN, R. P. & SANDBERG, A. L. (1970). *J. Immunol.* **104**, 320–328.

OVARY, Z. (1978). *Immunochemistry* **15**, 751–754.

OVARY, Z., BENACERRAF, B. & BLOCH, K. J. (1963). *J. Exp. Med.* **117**, 951–964.

PHIZACKERLEY, R. P., WISHNER, B. C., BRYANT, S. H., AMZEL, L. M., LOPEZ DE CASTRO, J. A. & POLJAK, R. J. (1979). *Mol. Immunol.* **16**, 841–850.

SAUL, F. A., AMZEL, L. M. & POLJAK, R. J. (1978). *J. Biol. Chem.* **253**, 585–597.